Acta Biomaterialia 9 (2013) 4754–4762

Contents lists available at SciVerse ScienceDirect

Acta Biomaterialia

journal homepage: www.elsevier.com/locate/actabiomat

Preparation of iron oxide nanoparticles stabilized with biomolecules: Experimental and mechanistic issues

Paula Nicolás [a], Martín Saleta [c], Horacio Troiani [c], Roberto Zysler [c], Verónica Lassalle [b,*], María Luján Ferreira [a]

[a] PLAPIQUI–UNS-CONICET, Camino La Carrindanga Km 7, B. Blanca, Bs As, Argentina
[b] INQUISUR–UNS-CONICET, Avda Alem 1253, 8000, B. Blanca, Bs As, Argentina
[c] Centro Atómico Bariloche—Instituto Balseiro, S. C. de Bariloche, RN, Argentina

ARTICLE INFO

Article history:
Received 12 June 2012
Received in revised form 18 September 2012
Accepted 28 September 2012
Available online 4 October 2012

Keywords:
Magnetic nanoparticles
Co-precipitation
Chitosan
Oleic acid
Bovine serum albumin

ABSTRACT

Nanoparticles (NPs) with magnetic properties based on magnetite (Fe_3O_4, MAG) modified with oleic acid (OA), chitosan (CS) and bovine serum albumin (BSA) have been prepared. A versatile method of synthesis was employed, involving two steps: (i) co-precipitation of MAG; and (ii) nanoprecipitation of macromolecules on as-formed MAG NPs. Experimental variables have been explored to determine the set of conditions that ensure suitable properties of NPs in terms of their size, functionality and magnetic properties. It was found that the presence of OA in Fe^{+2}/Fe^{+3} solutions yields MAG NPs with lower aggregation levels, while increasing initial amounts of OA may change the capability of NPs to disperse in aqueous or organic media by modifying the stabilization mechanism. Incorporation of CS was verified through Fourier transform IR spectroscopy. This biopolymer stabilizes NPs by electrostatic repulsions leading to stable ferrofluids and minimal fraction of recoverable solid NPs. BSA was successfully added to NP formulations, increasing their functionality and probably their biocompatibility. In this case too stable ferrofluids were obtained, where BSA acts as a polyelectrolyte. From the proposed methodology it is possible to achieve a wide range of NPs magnetically active intended for several applications. The required properties may be obtained by varying experimental conditions.

1. Introduction

Nanoscale magnetic structures offer great potential for advancements in electronics, optioelectronics, magnetic storage, biocatalysis, environmental remediation and biomedical applications [1,2]. Nanosized magnetic materials display properties that differ from their respective bulk material counterparts. Size and surface effects dominate the magnetic behavior of magnetic nanoparticles (NPs) [3].

Iron oxide-based NPs may be prepared by a number of methods [4], such as co-precipitation of an aqueous solution of Fe^{+2}/Fe^{+3} ions using a base as precipitation agent [5,6], sol–gel techniques [7], sonochemistry [8], colloidal methods [9], pyrolysis reaction [10], etc.

A difficulty associated with the preparation of magnetic NPs is that these particles have large surface area-to volume ratios and thus tend to aggregate to reduce their surface energy. Specifically, magnetic metal oxide surfaces have extremely high surface energies (>100 dyn cm^{-1}) that make the production of NPs very challenging. In addition, magnetic dipole–dipole attractions between particles enhance the difficulties experienced in their production in comparison to non-magnetic NPs. Prevention and/or minimization of particle agglomeration is one of the critical obstacles to be overcome in producing stable magnetic NPs irrespective of whether physical grinding or chemical reaction is used in their fabrication [11]. A wide range of monomers, polymers and organic materials may be used for stabilization purposes [12,13], where the balance between steric and electrostatic repulsive forces is crucial. Oleic acid (OA) is a commonly used surfactant to stabilize magnetic NPs synthesized by the traditional co-precipitation method. Some studies have demonstrated the strong chemical bond formed between carboxylic acid, amorphous iron and amorphous iron oxide NPs [14–17]. The OA layer disperses the NPs and prevents them from forming large clusters due to magnetic dipole–dipole interactions [18]. Gyergyek et al. reported that bonding of OA to magnetite (Fe_3O_4, MAG) causes a clear shift from a strong electron-donor to a weak electron-donor, whereas in the case of ricinoleic acid bonding on MAG a clear shift towards a weak electron-acceptor is evident [19].

* Corresponding author. Tel.: +54 0291 4595101 2835.
E-mail addresses: veronica.lassalle@uns.edu.ar, vlassalle@plapiqui.edu.ar (V. Lassalle).

1742-7061/$ - see front matter © 2012 Acta Materialia Inc. Published by Elsevier Ltd. All rights reserved.
http://dx.doi.org/10.1016/j.actbio.2012.09.040

Modification of magnetic NPs with polymers is other promising tool to achieve stable and non-aggregated particles [1,2,20,21].

Chitosan (CS) is a natural polymer with a high density of amine groups in its structure (these amines may be protonated depending on pH); it is biodegradable and provides excellent drug support, making it suitable, for instance, for biomedical applications [22]. It has enough reactive sites to bind Fe-based NPs, inducing their stabilization by several mechanisms [23–27].

Bovine serum albumin (BSA) is one of the most extensively studied proteins, thanks in particular to its structural homology with human serum albumin [28]. It is a small protein with a single polypeptide chain, which is cross-linked by 17 disulfide bonds [29]. BSA is used in biomedical research as a model for future applications of more complex medicines [30]. Hence, based on literature reports, BSA was selected as an additional modifier within this work, with a double purpose. The first was to supply extra biocompatibility to magnetic NPs regarding potential biomedical applications. It has been demonstrated, through in vivo assays, that polymeric BSA devices are able not only to increase biocompatibility but also to decrease the toxicity of certain drugs such as doxorubicin (an antitumoral drug). In this particular case it was also found that the presence of protein significantly increases the survivability of hepatoma H22 tumor-bearing mice, the animal model chosen for in vivo assays in Ref. [30]. The second purpose was to provide further functional groups (i.e. amino and carboxyl from protein) to these systems, increasing the possibilities of interaction with a wide range of substrates. The ability of BSA to bond different molecules has been well documented and interactions are not restricted to electrostatic ones. Hydrophobic forces can be established between the protein and suitable substrates [31].

The open literature contains a vast amount of information about the synthesis and modification of iron oxide-based NPs, and a great deal of work describes the use of co-precipitation as the synthesis methodology [4]. However, little has been published on the relationships between the principal experimental conditions used in these preparation methods and the final properties of magnetic NPs. Zhang et al. have published one of the few articles reporting the synthesis MAG NPs, based on a hydrothermal reaction using sodium bis(2-ethylhexyl) sulfosuccinate as a surfactant and hydrazine hydrate ($N_2H_4{\cdot}H_2O$) as a reductant [32]. The goal of the present work is to analyze experimental variables involved in the synthesis of magnetic NPs based on MAG coated with OA, CS and BSA. The aim is to provide not only stabilization of NPs but also biocompatibility and surface functionality in order to make them suitable for diverse biotechnological and biomedical applications. Two simple and low-cost methods have been integrated: co-precipitation to achieve MAG NPs; and nanoprecipitation to incorporate the CS and BSA [33]. Furthermore, the main goal is to characterize the prepared systems to evaluate their size, surface charge and magnetic properties, and to establish correlations between experimental variables and final properties of NPs, proposing mechanisms for interactions of MAG with different additives.

The novelty of this contribution is related to the studied system (i.e. MAG, OA, CS and BSA). Although each of these substrates has been employed previously to coat magnetic NPs, coating using a combination of them has not, to the best of our knowledge, been performed before. Furthermore, unlike most previous published work, we have included a study of the nature of the interactions with the substrate from a chemical viewpoint. The mechanistic aspects of the formation of magnetic NPs coated with various types of substrates have not been sufficiently studied and, in our opinion, are of utmost importance—firstly, to understand the final properties of NPs; and secondly, to be able to design specific and tailored particles for well-defined applications.

2. Experimental

2.1. Materials

OA was supplied by Anedra and CS (ChitoClear) by Primex (Iceland). Analytical-grade solvents provided by Dorwill (Argentina) were used in all the described procedures. BSA was supplied by Laboratorios Wiener (Argentina). Polyethylene glycol (PEG) was from Sigma.

2.2. Synthesis of magnetic nanoparticles

2.2.1. Co-precipitation of magnetite

MAG was synthesized by the co-precipitation method [34]. In brief 1.0862 g $FeCl_3{\cdot}6H_2O$ and 0.5965 g $FeSO_4{\cdot}7H_2O$ were dissolved in 33.3 ml distilled water. The solution was stirred at 70 °C under a N_2 atmosphere for 25 min. Then, 8.3 ml 5 M NaOH was added to precipitate the oxide. MAG formation from the mixture was allowed to proceed for 30 min. Modifications to the co-precipitation procedure were implemented by addition of OA and PEG. The selection of these stabilizers was based on the abundant literature on their use as effective stabilizers of magnetic NPs; and also considering their biocompatibility and biodegradability. Different stabilizer concentrations as well as different sequences of additions were employed and are detailed in Table 1.

The MAG NPs modified with OA will hereinafter be named MAGM; those containing both OA and PEG are named MAGMPEG.

2.2.2. Nanoprecipitation of chitosan on magnetic NPs

Acetone was used to precipitate CS. A suitable amount of MAGM was dispersed in acetone under sonication for 15 min. A solution of CS in acetic acid (50%), containing a convenient amount of biopolymer, was added to the MAGM mixture. In general, an average of three sequences of centrifugation (at 4000 rpm)/redispersion with distilled water were performed to remove residual acetic acid as well as residues of unlinked CS of very low molecular weight. The obtained sample is named MAGM8CS hereinafter.

To incorporate BSA an adequate concentration of protein was included in a dispersion containing 50 mg MAGM8 in 8.6 ml of acetone. The resulting dispersion was then added to the CS solution following the procedure described above.

2.3. Characterization

2.3.1. FTIR spectroscopy

Diffuse reflectance infrared Fourier transform spectroscopy (DRIFTS FTIR) was performed with a Thermo Scientific Nicolet 6700 spectrometer, which was used to record spectra in the range 4000–400 cm^{-1}. A few milligrams of the samples (~10–20 mg) were mixed in a mortar manually with near 50 mg of KBr powder. The mixture was placed in the sample unit of the DRIFTS FTIR spectrometer.

2.3.2. Electron microscopy

Scanning electron microscopy (SEM, LEO EVO 40-XVP, Tokyo, Japan), transmission electron microscopy (TEM, JEOL 100 CX II, Tokyo, Japan), and high-resolution TEM (Phillips, accelerating voltage of 200 kV) were used to examine the morphology of the carriers. The TEM samples were dispersed in water, dried at room temperature and placed on 200 mesh Cu grids. Samples to be analyzed by SEM were used as powder and metallized with Au in a sputter coater (SPI).

Table 1
Experimental conditions evaluated during co-precipitation of magnetite.

Sample name	Initial mass of stabilizer (mg)	Ratio MAG/stabilizer (w/w)	Sequence of reactant addition	Mass of solid nanoparticles recovered (mg)	Yield%
MAGM1	300	1/1	(1) NaOH (2) OA	300	50
MAGM3	580	0.86	NaOH and OA simultaneous	355	33
MAGM4	580	0.86	(1) OA (2) NaOH	695	64
MAGM5	580	0.86	(1) AO (2) NaOH	571	53
MAGMPEG	580 (AO) + 33 (PEG)	0.86	(1) NaOH (2) OA and PEG	708	64
MAGM8	1500	0.28	(1) OA (2) NaOH	518	26
MAGM9	3750	0.11	(1) OA (2) NaOH	519	12
MAGM10	6000	0.07	(1) OA (2) NaOH	613	10

2.3.3. X-ray diffraction

X-ray diffraction (XRD) analysis was performed to confirm the crystalline patterns of MAG in the different formulations. The assays were recorded by a Philips PW1710 diffraction spectrometer with a Cu anode and a curved graphite monochromator. The samples were employed as a powder with exception of MAGM8CS ferrofluid (FF). In this case, the sample was dried and then dispersed in a vaseline film that was supported on the sampler unit of the equipment.

2.3.4. Z potential (ζ) and hydrodynamic diameter (D_h) measurements

A Malvern Zetasizer was used to measure the Z potential and the average particle diameter. Dispersions of magnetic NPs were prepared at a concentration of 0.1 mg NPs/ml of distilled water to measure the Z potential. Dispersions with the same concentration of NPs were prepared using both distilled water and acetone as dispersants and were then ultrasonicated for 60 min to measure the average particle sizes (reported in nm).

2.3.5. Magnetic measurements

Magnetic properties were measured with a commercial vibrating sample magnetometer (LakeShore), at room temperature with a magnetic field in the −10 to +10 kOe range. The sample was used as a powder, weighed and then placed in the sampler unit for measurement.

2.3.6. Atomic emission spectroscopy

High-resolution inductively coupled plasma atomic emission spectroscopy (ICP-AES, Shimadzu 9000) was used to determine the composition of the NPs in terms of total Fe content. For these measurements, 1 mg of magnetic NPs was dissolved in 10 ml HCl 36% w/v.

3. Results and discussion

3.1. Effect of different experimental variables during co-precipitation of MAG

3.1.1. Influence of the presence of stabilizer

The incorporation of the selected stabilizers, OA, PEG and OA/PEG, into MAG was confirmed by DRIFTS analysis. The FTIR spectrum of iron oxide exhibited strong bands in the low-frequency region (1000–500 cm^{-1}) due to the iron oxide skeleton. The band located at 570 cm^{-1} is typical of MAG [35]. Evidence of OA incorporation can be seen in the spectra of MAGM1 and MAGMPEG by the presence of the COO^- band at ~1590 cm^{-1} and the signals associated with CH_2– groups of the alkyl OA chains [36].

The spectrum of MAGMPEG coincides with that of pure MAG. PEG is water soluble, and therefore it is possible that the polymeric chains weakly bonded to MAG were removed during the washings with distilled water. In the spectrum of MAGMPEG new bands located at 1558 (ν_s C–O); 3000–2846 (ν C–H); 961 and 904 (C=C) were observed.

In all explored cases the NPs presented the MAG crystalline pattern, according to XRD analysis (data not shown; see Supplementary material).

Morphological analysis by TEM reveals that particles are spherical in shape on the nanometer scale but form aggregates of variable sizes, depending on the incorporated modifier. MAG exhibits sizes near 10 nm with high aggregation, and the darkness of the image suggests that a unique phase (from iron oxide) is present. In the MAGM formulations the sizes are of the same order (13–20 nm) but better dispersion of the NPs is observed.

Agglomerated particles have a lower diffusion electrophoretic coefficient than dispersed single ones; therefore the diameter measured by dynamic light scattering (DLS) is higher than the one determined by TEM (see Table 2). NPs modified with OA are better dispersed in organic media, since their hydrodynamic volumes are lower than those found for unmodified MAG, pointing to lower aggregation of individual NPs in this solvent. Pure MAG NPs in organic media form aggregates, with high polydispersity index (PDI), bigger than the limit of detection of the equipment used here. These results correlate well with well-known postulated stabilization mechanism of OA molecules on MAG NPs [17,37]. Although the PEG is removed during the purification process, it stabilizes the MAG NPs, leading to well-dispersed particles in organic media [34].

The proposed stabilization mechanisms are supported by the Z potential (ζ) results, which are included in Table 2. Negatively charged NPs were obtained in all cases with minimal differences in ζ magnitude. The ζ data were measured from a suspension of MAG NPs in distilled water at almost neutral pH (6.8–7.4). The recorded ζ of raw MAG is due to hydroxyl groups that coordinate with Fe surface atoms. At certain pH values, the hydroxyl groups are deprotonated, leading to the observed negatively charged surface. As the OA molecules interact with MAG though COO^- groups, this stabilizer does not provide extra negative charge on the surface of the NPs. Therefore, the slight decrease in the magnitude of ζ potential can be attributed to partial covering of the MAG surface [37]. A similar justification explains the results when PEG is used as stabilizer.

3.1.2. Sequence of reactant incorporation

The sequence of reactant addition studied here is illustrated in Fig. 1a. DRIFTS spectra of MAGM1 and MAGM4 show characteristic

Table 2
Hydrodynamic diameter (nm) and Z potential (ζ, mV) of magnetite nanoparticles with different stabilizers.

	Hydrodynamic diameter (nm)				ζ (mV)
	Water	PDI	Acetone	PDI	
MAG	417	0.252	[a]	0.455	−8.48
MAGM1	319	0.301	95	0.211	−6.31
MAGMPEG	317	0.361	239	0.248	−8.95

[a] Measurement was not accurate. Sizes too large, exceeding the limit of detection of the equipment.

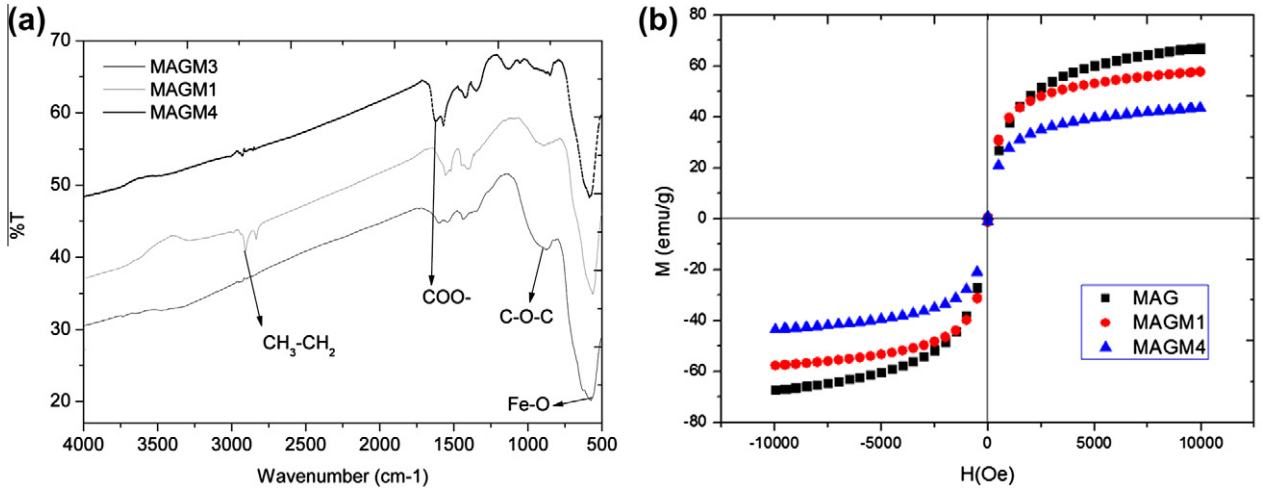

Fig. 1. (a) DRIFTS spectra of MAGM1, MAGM3 and MAGM4. (b) Magnetization curves at room temperature of MAGM1 and MAGM4.

bands of both OA and MAG. In the spectrum of MAGM3 the peaks related to the molecular structure of OA are almost absent (or weakly detected), and only the Fe–O band can be distinguished. This analysis suggests that the addition of NaOH simultaneously with the OA renders only MAG NPs without stabilizers linked to them.

SEM analysis of NPs arising from different addition sequences demonstrates that the aggregation of individual NPs is strongly dependent on this experimental parameter. In Fig. 2 photographs of the batch reaction are included with different sequences of NaOH/OA incorporation; microscopic analyses of the obtained products are also shown. The incorporation of OA after NaOH leads to highly agglomerated NPs, whereas when the stabilizer is added before alkali addition, the particles appear more disperse. In the case of simultaneous OA/NaOH addition, the morphology of the recovered solid matches corresponds to that of pure MAG. The observed differences can be explained in terms of the mechanism of formation of MAG by co-precipitation. The formation of iron oxides by this method involves two main steps: nucleation and crystal growth. Nucleation is controlled by the formation of a nucleus leading to the initial stage of particle formation. The number of nuclei must be increased, reducing the growth of the previously formed ones [38,39].

The presence of stabilizers, such as OA, in the Fe^{+2}/Fe^{+3} initial solution affects the crystal growth [40,41]. Ostwald ripening probably occurs, meaning that the formation of large particles is retarded while the formation of smaller ones is accelerated. The result is a shell–core structure with hydrophobic oleate chain as shell and hydrophilic ferric hydroxide and ferrous hydroxide as core. Ferric and ferrous hydroxides in the core are dehydrated, and finally MAGM crystals are obtained [11,41–43]. Fig. 3 shows a mechanism of OA incorporation and interaction with in situ forming MAG; the coordination nature of these interactions is obvious here. The incorporation of OA after the base addition is the most common way to incorporate this and other stabilizers [19,44]. The COO^- groups on OA form coordination bonds with the surface Fe on MAG NPs and with aggregates of them of various sizes. It is worth noting that the ability of OA to form coordination

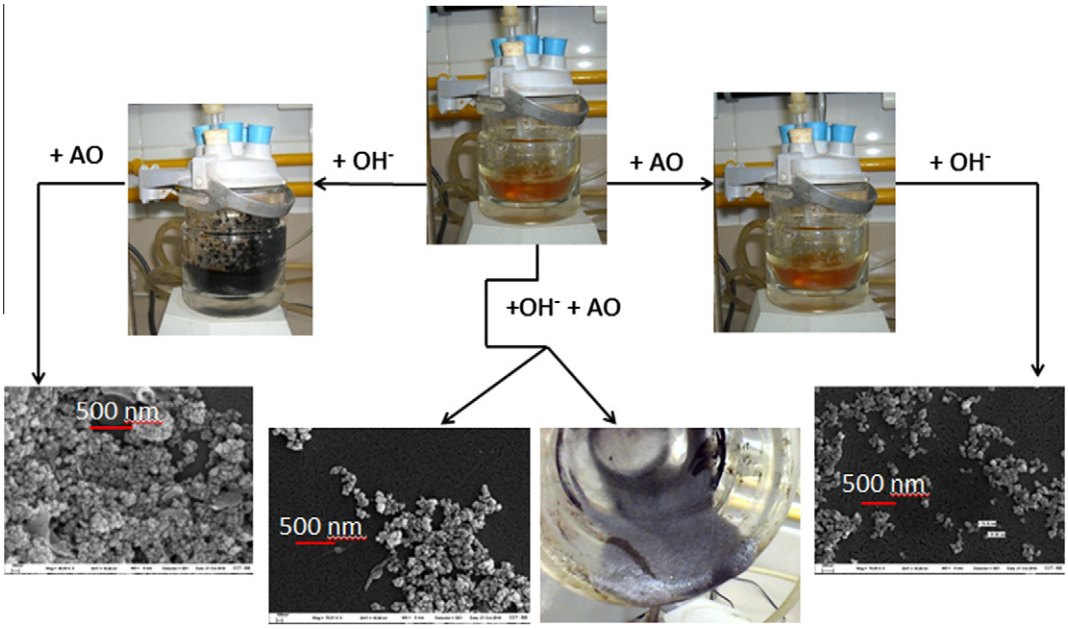

Fig. 2. Photograph of experimental steps involved in different sequences of reactant addition and SEM micrograph corresponding to the products obtained from each step.

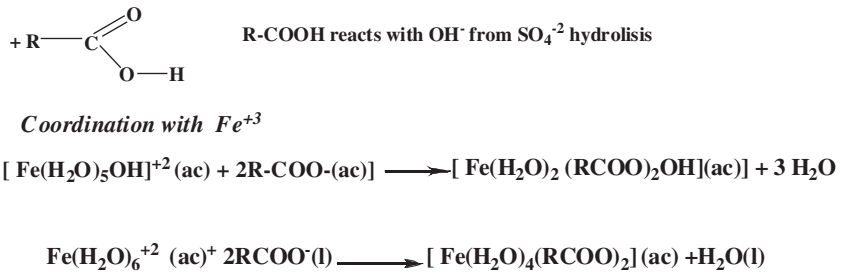

Fig. 3. Feasible mechanism for the formation of MAGM adding OA before alkali.

complexes with Fe^{+2}/Fe^{+3} species has been reported in the open literature, and FTIR spectroscopy has been used to examine these interactions [37,45–48].

Simultaneous addition of OA and NaOH results in different by-products (see Fig. 2). The FTIR analysis of the achieved grey foam (data not shown; see Supplementary material) demonstrated the presence of Fe^{+2}/Fe^{+3} associated with oleate, but also a band corresponding to Fe–O at ~570 cm^{-1}. The decanted solid was demonstrated to be pure MAG by both FTIR and SEM/TEM analysis. This sequence of reactant addition proved to be ineffective for the purposes of this work.

Magnetic characterization suggests that MAGM1 and MAGM4 exhibit superparamagnetism and satisfactory levels of magnetization saturation (Ms) (see magnetization curves included in Fig. 1b).

3.1.3. Concentration of oleic acid

Significant differences were found in terms of the surface charge when comparing formulations with different nominal amounts of OA. Fig. 4 shows the ζ values as a function of the amount of stabilizer added during co-precipitation. A decreasing proportional dependency was noted between the zeta potential and the OA concentration. This suggests that using low concentrations of OA resulted in COO^- groups (from OA) interacting with iron oxide surface and alkyl tails being exposed. Hence, the stabilization mechanism is steric hindrance repulsion. When the amount of OA increases, ζ goes drastically to very negative values. In these cases a double layer of OA is formed, meaning that a different stabilization mechanism is in operation [14,45]. The first layer is linked to the Fe surface by a coordination bond, while the second one is physically bonded to the first one though the alkyl groups establishing weak Van der Waals interactions. Consequently the hydrophilic COO^- groups are exposed to the surface, increasing the magnitude of ζ with negative sign.

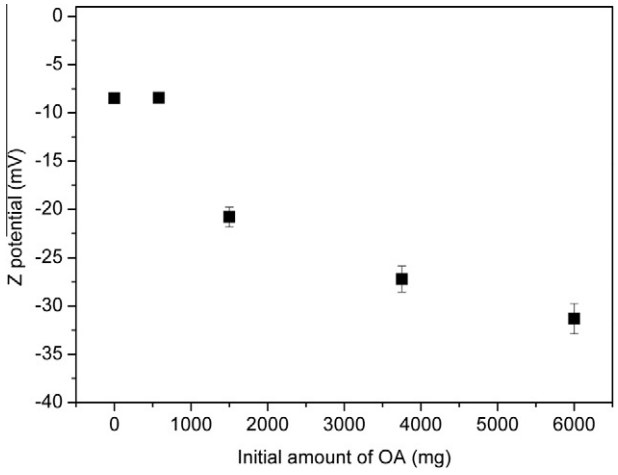

Fig. 4. Z potential (ζ, mV) as a function of the initial amount of OA (mg) added during co-precipitation.

Evidence of formation of OA bilayer can be also found by FTIR analysis. In Fig. 5a DRIFTS spectra of MAGM containing different concentrations of OA are recorded. Signals assigned to OA functional groups are found in all spectra, with increasing intensity as OA concentration grows. In particular, the band located at 1710 cm^{-1} that appears clearly in the MAGM10 spectrum, but is less clearly observed in the MAGM9 and MAGM8 spectra, is associated with the OA double layer [50]. This band is assigned to C=O groups of OA molecules that form the second layer and are physically bonded to the first one. Therefore free COO^- groups remain exposed on the NP surface, conferring the highly negative value of ζ. It is worth noting that FTIR signals from the first OA layer at near 1520 and 1450 cm^{-1} assigned to COO^- coordinated with Fe are seen in the spectra of MAGM with lower OA content.

The HRTEM image of MAGM8 in Fig. 6a shows a layer of OA surrounding a MAG core. The distance between the magnetic core (dark zone in Fig. 6a) and the end of the layer was found to be ~40 Å, which agrees with the approximate length of two OA molecules (assuming 20 Å per molecule). Hence, the morphological assays also confirm the proposed bilayer stabilization mechanism.

NPs prepared from low nominal amounts of OA (MAGM4) showed a magnetization saturation (Ms) of about 43.1 emu g^{-1} while in the case of MAGM10 this value falls to 19 emu g^{-1} [49]. A non-magnetic layer (dead layer) on the NP surface generated from stabilizer molecules interacting with surface Fe would be present, reducing the average magnetic moment of superparamagnetic NPs [50].

3.2. Nanoprecipitation of magnetic NPs on chitosan and chitosan–BSA

The formulation MAGM8 was chosen, using polymer (CS) and protein (BSA) as extra modifiers.

3.2.1. Modification of magnetic NPs with CS

The incorporation of CS into MAGM8 moieties was confirmed by FTIR-DRIFTS spectroscopy. Typical bands associated with biopolymer functional groups and those indicating formation of the iron oxide framework are clearly observed in the spectrum of MAGM8 CS-modified NPs, as shown in Fig. 5b.

During the nanoprecipitation procedure, CS was dissolved in acidic media (pH 4.5), leading to protonated NH_2 groups. The precipitation takes place by means of a CS non-solvent (acetone). During the purification process, a large fraction of the solid NPs formed a stable dispersion in water (a FF) and only a minimal fraction precipitated by means of a high-power Nd magnet.

Surface and size characterization of both products, solid NPs and FF, led to formulations that substantially differ in their chemical and surface properties. In Table 3, ζ, hydrodynamic diameter and Fe content (from MAG, measured by ICP-AES) are listed as a function of the kind of product obtained during nanoprecipitation.

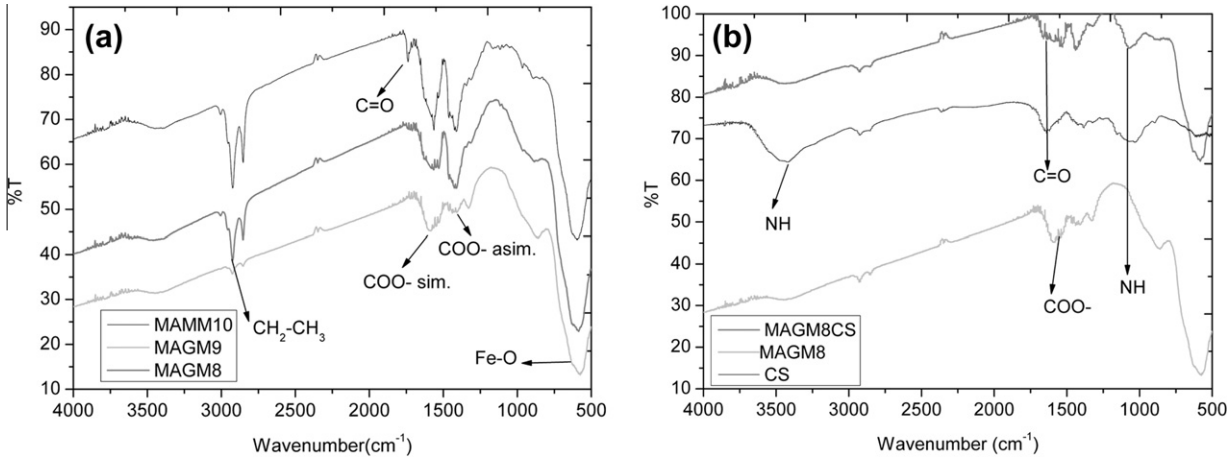

Fig. 5. DRIFTS spectra of (a) MAG modified with different OA concentrations; and (b) pure biopolymer, MAGM8 and MAGM8 modified with CS.

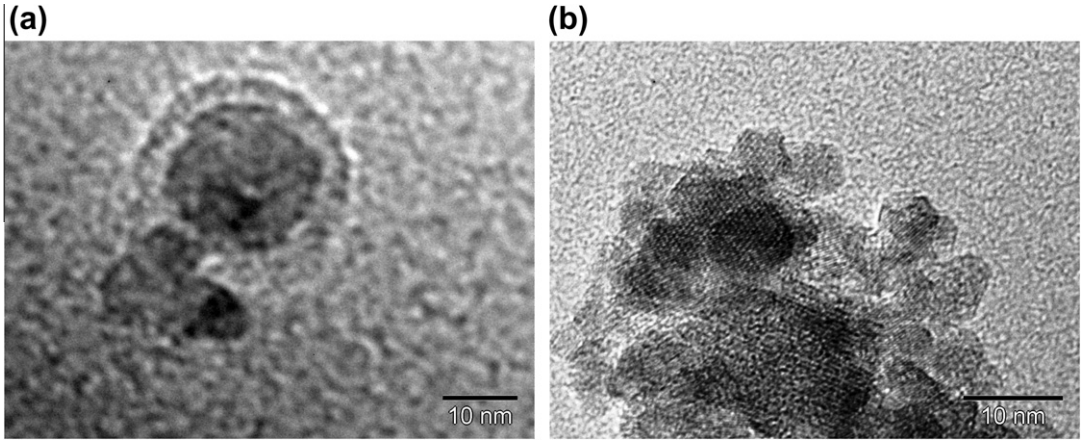

Fig. 6. HRTEM image of: (a) MAGM8; (b) MAGM8CS nanoparticles.

Table 3
Z potential (ζ, mV), hydrodynamic size and Fe content (from MAG) measured by ICP of MAGM8CS NPs and FF.

Products from nanoprecipitation	ζ, (mV)	Dh (nm) water	PDI	Mg Fe/mg NPs	Mg MAG/mg NPs
Solid MAGM8CS1	−3.26	1380	0.387	0.528	0.733
MAGM8CS 1 FF	+35.6	168.3	0.243	0.0560	0.078

Solid NPs show negative ζ value, suggesting that the amount of CS incorporated was not enough to completely cover the NP surface (see Table 3). The high positive value of ζ found for the FF indicates that most of CS was incorporated in this case, and positive surface charge may be assigned to protonated amino groups of the biopolymer exposed on the NP surface.

The magnitude of ζ is generally accepted as a marker for the stability of NP dispersions. High ζ values explain the stability of the FF at almost neutral pH with electrostatic repulsion as the stabilization mechanism [51,52].

HRTEM demonstrated the nanosize (10–30 nm) of these particles and also allowed lattice patterns corresponding to the spinel cubic structure of MAG to be distinguished (see Fig. 6b). The single-crystal nature of the particles is evidenced by the presence of crystalline planes in the HRTEM images with a single orientation for each NP [27].

A representation of the interactions between CS and MAG in both FF and CS-modified MAGM solid NPs is included in Fig. 7a and was based on results from different characterization techniques. Two dissimilar situations may be visualized. On the one hand, partial exchange of OA molecules adsorbed on MAG by the complex acetate (from acetic acid, which dissolves CS) results in protonated chitosan. Acetone (used as precipitating agent) in the presence of CS and acetate moieties partially removes OA molecules from the MAG surface. When the MAG particle size is big (because of aggregation of smaller particles), the exposed surface is different to that found in the case of smaller MAG particles and this surface remains almost "clean" with a fraction of the total initial amount of OA incorporated into MAG. As a result it may be recovered as solid NPs.

On the other hand, when MAG particle size is small, the exposed surface is completely covered by the complex acetate-protonated chitosan. This material exposes the protonated NH_2 (NH_3^+) groups to aqueous solution in such a way that strong electrostatic repulsions are present and a stable FF is obtained. The acetic acid concentration used to prepare the CS solution plays a key role in achieving this FF because of the proposed exchange between OA and acetate ions at the MAG surface, which form Lewis acid–base

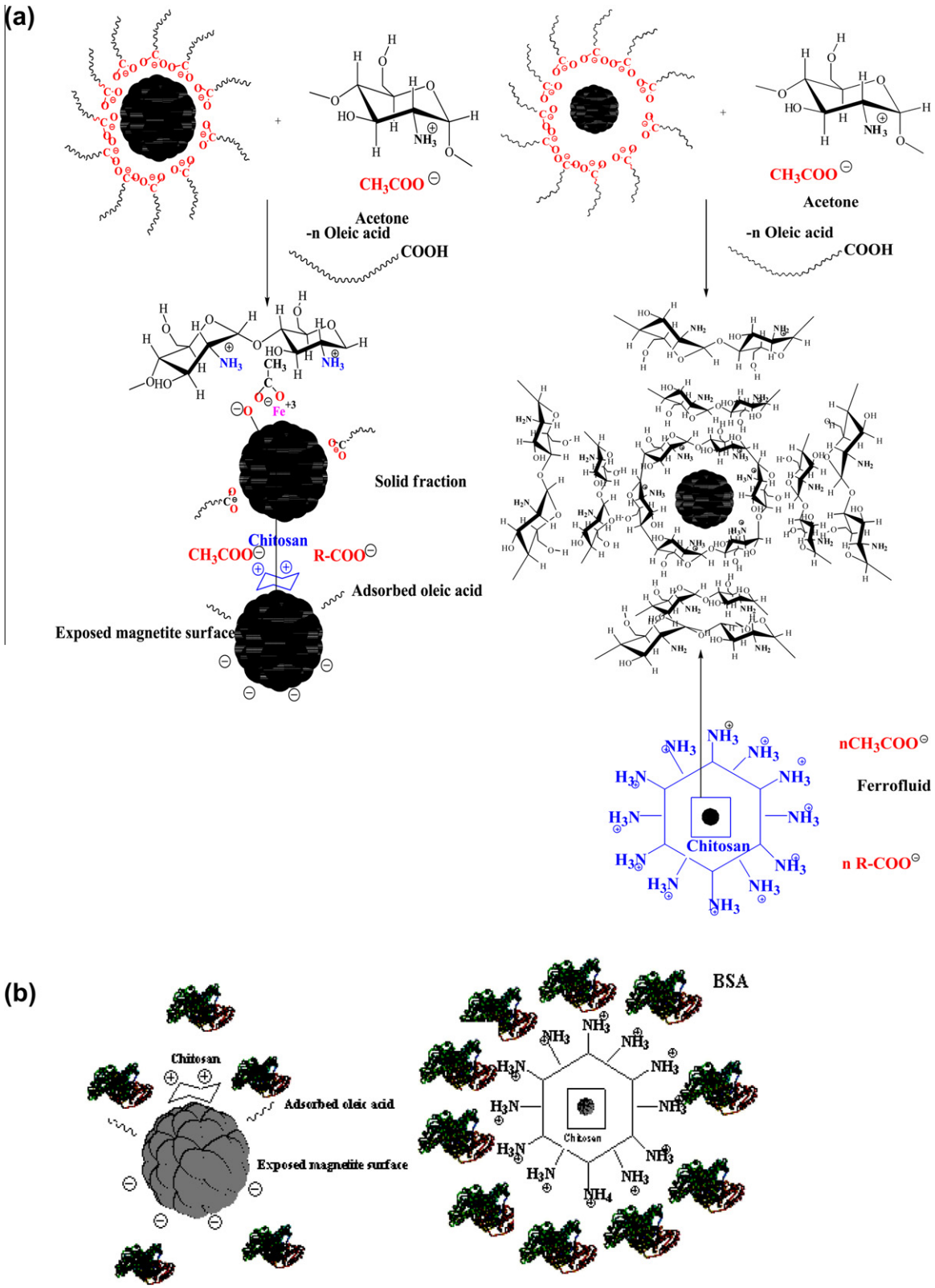

Fig. 7. (a) Feasible mechanism of interaction between MAGM and CS. (b) Feasible mechanism of interaction between BSA and MAGM8 and CS.

complexes with surface Fe (see Fig. 7a). To support this hypothesis, additional experiments were carried out using CS solution with lower acetic acid concentration, and FF was not produced. Furthermore, the percentage of OA linked to MAG in MAGM8 NPs was near 50% w/w before CS addition. After biopolymer incorporation the final percentage of additives (OA + Acetate − CS) on material recovered as a solid was about 28% w/w, confirming the partial removal of OA from MAG surface.

Regarding the magnetic properties, superparamagnetic character was found in formulations prepared from MAGM8 and CS, with

values of saturation magnetization of the same order as the MAGM8 precursor (data not shown; see Supplementary material).

3.2.2. Modification of magnetic NPs with BSA

BSA was incorporated during the nanoprecipitation of CS, without other stabilizers or additives. The formulation selected for this purpose was MAGM8CS. Different BSA concentrations (5, 15 and 25 mg BSA/50 mg MAGM8) were used, and it was found that only the lowest allows recovery of even a small amount of solid NPs. Using 15 and 25 mg BSA/50 mg MAGM8 stable dispersions such as FFs were generated without isolation of solid NPs even when the solutions were exposed to a high-power Nd magnet.

The ζ of MAGM8CS NPs decreases with the incorporation of BSA, as shown in Table 4. An almost constant ζ value is obtained using high protein concentrations. Protein-loaded NPs show lower sizes than the MAGM8CS precursor. A reduction of near 50% in hydrodynamic diameter is noted, with comparable size values between formulations containing increasing amounts of protein (see Table 4). BSA-modified NPs are completely different from MAGM8CS NPs in shape and size, as demonstrated by the TEM images included in Fig. 8. TEM sizes are in agreement with those measured by DLS, probably due to a reduction in aggregation in aqueous dispersion as a consequence of protein incorporation [53]. Possible mechanisms for BSA incorporation into NPs are included in Fig. 7b, based on data from characterization techniques. Initially, hydrophobic and H bonding interactions could be established between protein and MAG surface free of OA molecules [50,51]. Then, protonated amino groups of CS are partially neutralized by functional negatively charged lateral protein groups [54]. Electrostatic interactions are the driving force binding BSA to CS, forming MAGMCS-BSA stable FF, especially at pH 4.5 (solution of CS) [55,56]. Therefore BSA almost completely covers the surface of MAGM8CS NPs. The protein interacts strongly with CS surface in such a way that BSA becomes a polyelectrolyte with a particular exposed surface to the solution, stabilizing the NPs by electrostatic repulsion, and producing only FFs.

Table 4
Hydrodynamic diameter (nm) and Z potential (ζ, mV) of MAGM8CS modified with different amounts of BSA.

Sample	pH	ζ (mV)	Dh (nm)	PDI
MAGM8CS	6.6	25.7	678	0.376
MAGM8/CS/BSA 5	6.79	8.52	356.1	0.746
MAGM8/CS/BSA 15	7.00	2.36	399	0.236
MAGM8/CS/BSA 25	6.80	3.38	350	0.204
CS/BSA[a] 167/5 p/p	6.6	36.6	3913	0.438
BSA (5 mg ml^{-1})	7.2	−26.6	–	–

[a] Physical mixture.

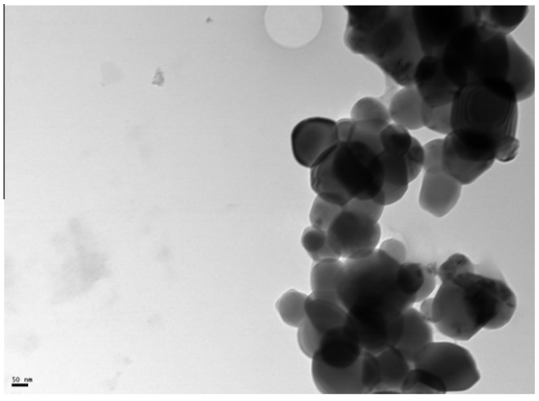

Fig. 8. TEM images of NPs modified with BSA.

The magnetic properties of NPs containing BSA were qualitatively verified by exposing them to a high-power Nd magnet. To do this, stable dispersions of such NPs in distilled water were prepared and placed in contact with the magnet. The migration of the particles to the magnet was observed and was taken as proof of the magnetic character of these formulations. As was mentioned earlier, magnetic characterization of NPs coated with CS, included as Supplementary material, revealed that they were superparamagnetic with acceptable magnetization saturation values. Considering that the procedure to incorporate BSA is almost similar to the one performed to incorporate CS, it is expected that the magnetic properties should be roughly comparable.

4. Concluding remarks

A study on the experimental conditions required for the synthesis of iron oxide NPs modified with polymeric and non-polymeric additives has been developed, and provides a novel view of this process. A stabilizer is necessary to obtain relatively stable NPs prepared by the co-precipitation method. The order of addition of additives and alkali solution plays a key role during the co-precipitation step. The subsequent modification of NP-loaded OA with CS was successful achieved by the nanoprecipitation method. Two products were obtained by this procedure: solid NPs mainly constituted by iron oxide; and a stable dispersion in aqueous media comprising mainly biopolymer with a minimal amount of MAG. Both products exhibited satisfactory magnetic properties. The incorporation of BSA into NPs resulted in FFs that were stable for more than 3 months.

A simple, low-cost and versatile protocol to prepare functionalized and non-toxic magnetic NPs has been reported. Using these procedures, it is possible to obtain tailored properties of magnetic NPs suitable for a wide range of applications.

Acknowledgements

The authors acknowledge the financial support from CONICET (Argentina) and the economic support from PICT 0788-2010 (ANPCyT, Argentina) and the PGI No. 24/Q016 (UNS, Argentina).

Appendix A. Figures with essential color discrimination

Certain figures in this article, particularly Figs. 1, 2, and 7, are difficult to interpret in black and white. The full color images can be found in the on-line version, at http://dx.doi.org/10.1016/j.actbio.2012.09.040.

Appendix B. Supplementary data

Supplementary data associated with this article can be found, in the online version, at http://dx.doi.org/10.1016/j.actbio.2012.09.040.

References

[1] Oha JK, Jong Myung Park JM. Iron oxide-based superparamagnetic polymeric nanomaterials: design, preparation, and biomedical application. Prog Polym Sci 2011;36:168–89.
[2] Dias A, Hussain A, Marcos A, Roque A. A biotechnological perspective on the application of iron oxide magnetic colloids modified with polysaccharides. Biotechnol Adv 2011;29:142–55.
[3] Vekas L, Bica D, Avdeev M. Magnetic nanoparticles and concentrated magnetic nanofluids: synthesis, properties and some applications. Chin Particuol 2007;5:43–9.
[4] Lassalle VL, Avena M, Ferreira ML. A review of the methods of magnetic nanocomposites synthesis and their applications as drug delivery systems and immobilization supports for lipases. Curr Trends Polym Sci 2009;13:37–67.

[5] Wu JH, Ko SP, Liu HL, Kim SS, Ju JS, Kim YK. Sub 5 nm magnetite nanoparticles: synthesis, microstructure, and magnetic properties. Mater Lett 2007;61:3124–9.
[6] Fried T, Shemer G, Markovich G. Ordered two dimensional arrays of ferrite nanoparticles. Adv Mater 2001;13:1158–61.
[7] Xu H, Yang W, Fu K, Du Y, Sui J, Chen Y, et al. Preparation and magnetic properties of magnetite nanoparticles by sol–gel method. J Magn Magn Mater 2007;309:307–11.
[8] Vijaya R, Koltypin Y, Cohen Y, Cohen Y, Aurbach D, Palchik O, et al. Preparation of amorphous magnetite nanoparticles embedded in polyvinyl alcohol using ultrasound radiation. Mater Chem 2000;10:1125–9.
[9] Martínez M, Espinosa R, Pérez J, Arenas A. Synthesis of magnetite (Fe_3O_4) nanoparticles without surfactants at room temperature. Mater Lett 2007;61:4447–51.
[10] Chiu W, Radiman S, Abdullah M, Khiew P, Huang N, Abd-Shukor R. One pot synthesis of monodisperse Fe_3O_4 nanocrystals by pyrolysis reaction of organometallic compound. Mater Chem Phys 2007;106:231–5.
[11] Lifen S, Paul L, Hatton A. Bilayer surfactant stabilized magnetic fluids: synthesis and interactions at interfaces. Langmuir 1999;15:447–53.
[12] Gupta A, Gupta M. Synthesis and surface engineering of iron oxide nanoparticles for biomedical applications. Biomaterials 2005;26:3995–4021.
[13] Laurent S, Forge D, Port M, Roch A, Robic C, Vander L. Magnetic iron oxide nanoparticles: synthesis, stabilization, vectorization, physicochemical characterizations, and biological applications. Chem Rev 2008;108:2064–110.
[14] Qiang L, Chao L, Fei Y, Shangying L, Jian X, Dejun S. Synthesis of bilayer oleic acid-coated Fe_3O_4 nanoparticles and their application in pH-responsive Pickering emulsions. J Colloid Interface Sci 2007;310:260–9.
[15] Wu N, Fu L, Su M, Aslam M, Wong K, Dravid V. Interaction of fatty acid monolayers with cobalt nanoparticles. Nano Lett 2004;4:383–6.
[16] Kataby G, Cojocaru M, Prozorov R, Gedanken A. Coating carboxylic acids on amorphous iron nanoparticles. Langmuir 1999;15:1703–8.
[17] Ingram D, Kotsmar C, Yoon K, Shao S, Huh Ch, Bryant S, et al. Superparamagnetic nanoclusters coated with oleic acid bilayers for stabilization of emulsions of water and oil at low concentration. J Colloid Interface Sci 2010;351:225–32.
[18] Tomitaka A, Koshi T, Hatsugai S, Yamada T, Takemura Y. Magnetic characterization of surface-coated magnetic nanoparticles for biomedical application. J Magn Magn Mater 2011;323:1398–403.
[19] Gyergyek S, Makovec D, Drofenik M. Colloidal stability of oleic- and ricinoleic-acid-coated magnetic nanoparticles in organic solvents. J Colloid Interface Sci 2011;354:498–505.
[20] Chen K, Zhu Y, Zhang Y, Li L, Lu Y, Guo X. Synthesis of magnetic spherical polyelectrolyte brushes. Macromolecules 2011;44:632–9.
[21] Sun J, Zhou S, Hou P, Yang Y, Weng J, Li X, et al. Synthesis and characterization of biocompatible Fe3O4 nanoparticles. J Biomed Mater Res Part A 2007;80A:333–41.
[22] Cruzat C, Peña O, Meléndrez M, Díaz-Visurraga J, Cárdenas G. Synthesis, characterization and properties of magnetic colloids supported on chitosan. Colloid Polym Sci 2011;289:21–31.
[23] Podzus P, Daraio M, Jacobo S. Chitosan magnetic microspheres for technological applications: preparation and characterization. Phys B 2009;404:2710–2.
[24] Debrassi A, Burger C, Rodrigues C, Nedelko N, Waniewska A, Dłużewski P, et al. Synthesis, characterization and in vitro drug release of magnetic *O*-carboxymethylchitosan-*N*-benzyl nanoparticles loaded with indomethacin. Acta Biomater 2011;7:3078–85.
[25] Chen J, Yang P, Ma Y, Wu T. Characterization of chitosan magnetic nanoparticles for in situ delivery of tissue plasminogen activator. Carbohydr Polym 2011;84:364–72.
[26] Fan L, Zhang Y, Luo CH, Lu F, Qiu J, Sun M. Synthesis and characterization of magnetic β-cyclodextrin–chitosannanoparticles as nano-adsorbents for removal of methyl blue. Int J Biol Macromol 2012;50:444–50.
[27] Kuo CH, Liu Y, Chang CH, Chen J, Chang CH, Shieh CH. Optimum conditions for lipase immobilization on chitosan-coated Fe_3O_4 nanoparticles. Carbohydr Polym 2012;87:2538–45.
[28] Peters T. Serum albumin. Adv Protein Chem 1985;37:161–245.
[29] Wang J, Wang Y, Gao J, Hu P, Guan H, Zhang L, et al. Investigation on damage of BSA molecules under irradiation of low frequency ultrasound in the presence of Fe^{III}-tartrate complexes. Ultrason Sonochem 2009;16:41–9.
[30] Lameiro M, Lopes A, Martins L, Alves P, Melo E. Incorporation of a model protein into chitosan-bile salt microparticles. Int J Pharm 2006;312:119–30.
[31] Jianing Q, Ping Y, Fen H, Chuiliang Y, Chong H. Nanoparticles with dextran/chitosan shell and BSA/chitosan core—doxorubicin loading and delivery. Int J Pharm 2010;393:177–85.
[32] Yan H, Zhang J, You CH, Song Z, Yu B, Shen Y. Influences of different synthesis conditions on properties of Fe_3O_4 nanoparticles. Math Chem Phys 2009;113:46–52.
[33] Lassalle V, Ferreira M. Nano and microespheres based on polylactide (PLA) polymers and copolymers: an overview of their characteristics as a function of the obtention method. Macromol Biosci 2007;7:767–83.
[34] Gaihre B, Khil M, Lee D, Kim H. Gelatin-coated magnetic iron oxide nanoparticles as carrier system: drug loading and *in vitro* drug release study. Int J Pharm 2009;365:180–8.
[35] Nyquist R, Kagel R. Infrared spectra of inorganic compounds. New York: Academic Press; 1971. p. 25.
[36] Rocchiccioli-Deltcheff C, Frank R, Cabuil V, Massart R. Surfacted ferrofluids: interactions at the surfactant-magnetic iron oxide interface. J Chem Res 1987;5:126–7.
[37] Zhang L, He R, Gu H. Oleic acid coating on the monodisperse magnetite nanoparticles. Appl Surf Sci 2006;253:2611–7.
[38] Zhang L, He R, Gu H. Synthesis and kinetic shape and size evolution of magnetite nanoparticles. Mater Res Bull 2006;41:260–7.
[39] Sun Z, Su F, Forsling W, Samskog P. Surface characteristics of magnetite in aqueous suspension. J Colloid Interface Sci 1998;197:151–9.
[40] Casula M, Jun Y, Zaziski J, Chan E, Corrias A, Alivisatos AP. The concept of delayed nucleation in nanocrystal growth demonstrated for the case of iron oxide nanodisks. J Am Chem Soc 2006;128:1675–82.
[41] Kim D, Mikhaylova M, Zhang Y, Muhammed M. Protective coating of superparamagnetic iron oxide nanoparticles. Chem Mater 2003;15:1617–27.
[42] Qu S, Yang H, Ren D, Kan S, Zou G, Li D, et al. Magnetite nanoparticles prepared by precipitation from partially reduced ferric chloride aqueous solutions. J Colloid Interface Sci 1999;215:190–2.
[43] Liu X, Kaminski M, Guan Y, Chen H, Liu H, Rosengart A. Preparation and characterization of hydrophobic superparamagnetic magnetite gel. J Magn Magn Mater 2006;306:248–53.
[44] Koshi A, Hatsugai S, Yamada S, Takemura Y. Magnetic characterization of surface-coated magnetic nanoparticles for biomedical application. J Magn Magn Mater 2011;323:1398–403.
[45] Yang K, Peng H, Wen Y, Li N. Re-examination of characteristic FTIR spectrum of secondary layer in bilayer oleic acid-coated Fe_3O_4 nanoparticles. Appl Surf Sci 2010;256:3093–7.
[46] Korolev V, Ramazanova A, Blinov A. Adsorption of surfactants on superfine magnetite. Russ Chem Bull 2002;51:2044–9.
[47] Shen L, Laibinis P, Hatton T. Bilayer surfactant stabilized magnetic fluids: synthesis and interactions at interfaces. Langmuir 1999;15:447–53.
[48] Nakamoto K. Infrared and Raman spectra of inorganic and coordination compounds. New York: John Wiley; 1997.
[49] Kodama R, Berkowitz E, McNiff J, Foner C. Surface spin disorder in $NiFe_2O_4$ nanoparticles. Phys Rev Lett 1996;77:394–7.
[50] Kaiser R, Miskolczy G. Magnetic properties of stable dispersions of subdomain magnetite particles. J Appl Phys 1970;41:1064–72.
[51] Belessi V, Zboril R, Tucek J, Mashlan M, Tzitzios V, Petridis D. Ferrofluids from magnetic-chitosan hybrids. Chem Mater 2008;20:3298–305.
[52] Zhua A, Yuan L, Liao T. Suspension of Fe_3O_4 nanoparticles stabilized by chitosan and *o*-carboxymethylchitosan. Int J Pharm 2008;350:361–8.
[53] Lynch S, Dawson K. Protein–nanoparticle interactions. Nano Today 2008;3:40–7.
[54] Fenoglio I, Fubini B, Ghibaudi E, Turci F. Multiple aspects of the interaction of biomacromolecules with inorganic surfaces. Adv Drug Deliv Rev 2011;63:1186–209.
[55] Li X, Chen M, Yang W, Zhou Z, Liu L, Zhang Q. Interaction of bovine serum albumin with self-assembled nanoparticles of 6-*O*-cholesterol modified chitosan. Colloid Surf B 2012;92:136–41.
[56] Boeris V, Farruggia B, Pico G. Chitosan–bovine serum albumin complex formation: a model to design an enzyme isolation method by polyelectrolyte precipitation. J Chromatogr B 2012;878:1543–8.